Mater. Res. Soc. Symp. Proc. Vol. 1520 © 2012 Materials Research Society
DOI: 10.1557/opl.2012.1690

Variation of Hardness and Modulus across the Thickness of Zr-Cu-Al Metallic Glass Ribbons

Z. Humberto Melgarejo[1], J.E. Jakes[2], J. Hwang[1,*], Y.E. Kalay[3,**], M.J. Kramer[3], P.M. Voyles[1,4], D.S. Stone [1,4]

[1]Materials Science Program, University of Wisconsin-Madison, Madison, WI 53706, U.S.A.
[2]Performance Enhanced Biopolymers, United States Forest Service, Forest Products Laboratory, Madison, WI 53726, U.S.A.
[3]Ames Laboratory (DOE), Ames, Iowa 50011, USA and Department of Materials Science and Engineering, Iowa State University, Ames, IA 50011, U.S.A.
[4] Department of Materials Science and Engineering, and Materials Science Program, University of Wisconsin-Madison, Madison, WI 53706, U.S.A.

*current address: Materials Department, University of California, Santa Barbara, Santa Barbara, CA 93106-5050, U.S.A.
**current address: Department of Metallurgical and Materials Engineering, Middle East Technical University, Ankara, 06800 Turkey.

ABSTRACT

We investigate through-thickness hardness and modulus of $Zr_{50}Cu_{45}Al_5$ metallic glass melt-spun ribbon. Because of their thinness, the ribbons are challenging to measure, so we employ a novel nanoindentation based-method to remove artifacts caused by ribbon flexing and edge effects. Hardness and modulus vary approximately linearly across the thickness but, unlike bulk ingots, the side of the ribbon that cooled most quickly had the highest hardness and modulus. This “inverse” variation may be caused by the fast-moving solidification front, which might conceivably, for instance, push free volume in advance of it. Annealing near T_g causes both hardness and modulus to increase and become more uniform across the thickness.

INTRODUCTION

Bulk metallic glasses (BMGs) are a promising class of materials for structural applications, especially at very small dimensions [1]. Large BMG ingots have higher hardness and modulus in the center than near the surface [2, 3], which is attributed to differences in free volume caused by different cooling rates during solidification [3]. Plummer et al. [2] demonstrated that this effect depends on sample size and glass fragility index. Melt spun ribbons have even more extreme cooling rates than ingots. Ribbons have been reported to have lower hardness and modulus than ingots, favored by the difference in cooling rates and free volumes [4], but this result has been questioned as an artifact arising from the small ribbon thickness [5].

In the present work, we report measurements of hardness and elastic modulus across thicknesses of $Zr_{50}Cu_{45}Al_5$ as-spun and structurally relaxed ribbons using nanoindentation, corrected for the effects of thin ribbon geometry using rigorous techniques we have developed [6, 7]. We observe that hardness and modulus vary approximately linearly across the thickness, but the slope is opposite of cast bulk ingots: as opposed to ingots the surface that solidified at highest cooling rate has higher hardness and modulus. During annealing both the hardness and modulus rise, but their slopes across the specimens diminish. Careful nanoindentation measurements may provide a more sensitive probe of structural differences and structural relaxation in quenched ribbons than differential scanning calorimetry (DSC), including the capability for spatially resolved measurements.

EXPERIMENT

$Zr_{50}Cu_{45}Al_5$ (at.%) ribbons (T_g=403 °C) about 50 μm thick were produced by Cu block single melt spinning technique with 25 m/s wheel speed under Ar atmosphere using the same method published previously [8]. We studied the as-spun ribbon, three ribbons annealed at 300°C (0.85 T_g) for 10, 20, and 60 minutes, respectively, and a ribbon annealed at 435°C (1.05 T_g) for 2 min. Prior to heat treatment specimens were encapsulated under high purity N_2 atmosphere in a glove box. Annealing experiments were performed by using a TA Instrument Q100 differential scanning calorimeter (DSC) with ultra high purity (99.999%) nitrogen purge and heating and cooling rates of 20°C/minute. All specimens were verified glassy by TEM and x-ray diffraction. DSC curves for as-quenched and annealed ribbons are shown in Fig. 1, revealing evidence of different levels of structural relaxation depending on annealing time and temperature. The specimen annealed at 435°C for 2 minutes appears fully relaxed, although nanoindentation measurements, described below, suggest otherwise. Structural characterization of these samples has also been performed [9].

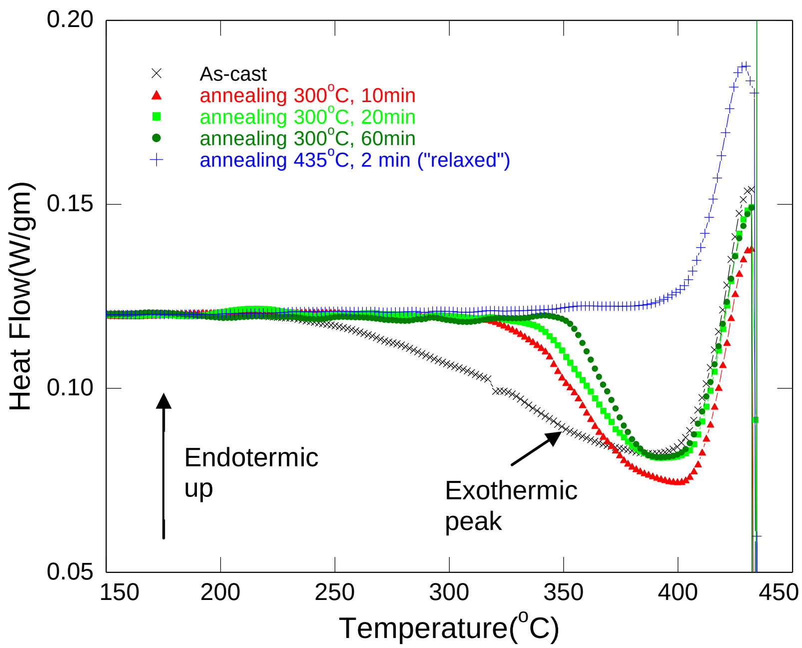

Figure 1. DSC Heat evolution analysis for $Zr_{50}Cu_{45}Al_5$ ribbon MG subjected to different annealing treatments.

As shown in inset of Figure 1, samples were clamped between brass bars held in place by screws without adhesive, then polished to an 0.05 μm alumina finish and tested (tests on samples mounted in epoxy were complicated by creep of the epoxy). We measured hardness and modulus using a Hysitron Triboindenter with a Berkovich tip. The usual definitions are used: Meyer hardness (H) is load/projected area, and modulus is $E/(1-\nu^2)$, with E as Young's modulus, and ν as Poisson's ratio.

Methods for measuring properties to remove artifacts caused by extreme specimen thinness were invented by Jakes et al [6, 7]. These artifacts are caused by the flexing of the specimen and by elastic discontinuities such as the ribbon/brass interface and the free edge of the ribbon when a gap exists between ribbon and brass. Provided indents are not placed too close to the specimen edge, the artifacts derive entirely from added elastic displacements, which enter through a structural compliance, C_s. C_s increases near a free edge, but its influence can be removed by measuring the areas of indents directly rather than relying on indenter shape calibration, and by constructing each indent using a series of load-hold-unload-hold segments reaching progressively higher load. This latter procedure allows the experimenter to isolate and remove displacements arising from C_s. For the present experiments each nanoindent consisted of 10 segments, each with 2 s loading, 3 s hold at constant load, 1 s unloading, and 1 s hold at partial unloading. Reported hardness is at 10 mN maximum load obtained from the final segment. Drift was measured at 3 mN load for 60 s following the final unloading segment. The indent areas were measured from SEM images acquired on a LEO 1530 FESEM. An array of multiload indents is shown in-Fig. 2

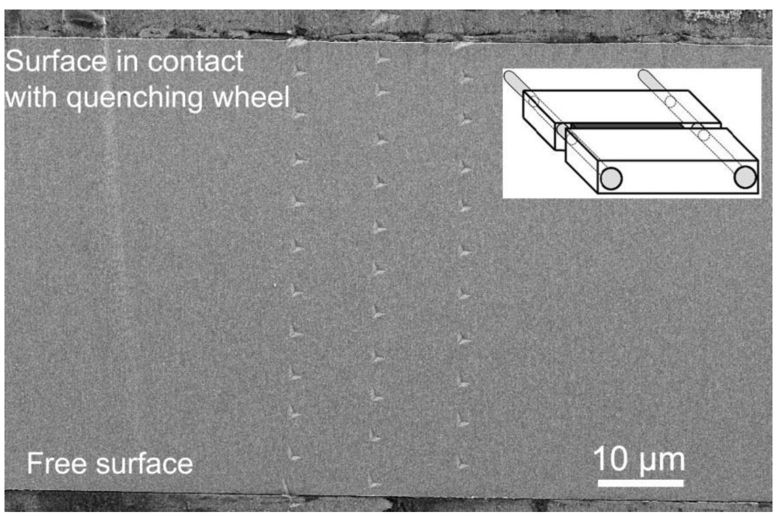

Figure 2. SEM image of an array of multiload indents performed along the cross section of the as-cast $Zr_{50}Cu_{45}Al_5$ ribbon MG (inset, illustration of a ribbon clamped between brass bars using screws).

RESULTS AND DISCUSSION

Usual nanoindentation procedure [10] relies on hardness and modulus readings put out by the instrument based on the penetration depth and indenter shape. These "uncorrected data" fail to account for C_s and pileup [11]. We compare uncorrected data with data obtained using the corrected method in Fig. 3. In the central region of the specimen both methods show the same trends in modulus and hardness versus position, but near the edges the uncorrected modulus data decrease dramatically. This effect is the artifact caused by C_s, so it is absent in the corrected data. The artifact is present but smaller in the uncorrected hardness data [12] and gone in the corrected hardness. Hardness and modulus vary approximately linearly across the specimen thickness. Fig. 3 shows the best fit lines to the data. The residuals (not shown) suggest that the data may fall below the fit lines very near the surfaces. Pileup causes the uncorrected hardness and modulus data to appear higher than they actually are.

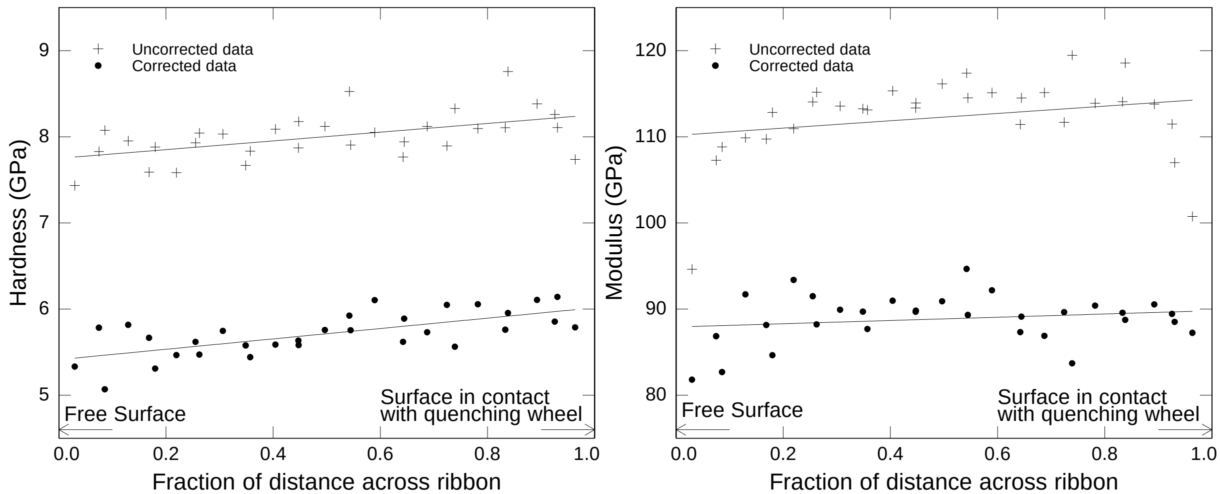

Figure 3. Corrections of hardness and modulus of the $Zr_{50}Cu_{45}Al_5$ as-pun ribbon by accounting for pile up and structural compliance.

The corrected data show clear trends to higher and more uniform hardness during annealing near T_g, as illustrated Fig. 4. The ribbons approach full uniformity from 60 minutes relaxation at 300°C. Data at 300°C suggest that the gradient in modulus across the ribbon might rise initially before falling during annealing. However, after 2 minutes at 435°C the properties still vary across the ribbon even though the DSC data suggest this ribbon is fully relaxed, signifying that nanoindentation is the more sensitive measure of structural relaxation. Table I summarizes the increase in hardness and modulus measured at midpoint across the ribbons for different annealing treatments. Differences in hardness and modulus between surface in contact with wheel and the free surface based on a linear fit are evaluated as well. Side contacting quenching wheel has higher properties.

Like our ribbons, when ingots are annealed their hardnesses and moduli increase and become more uniform across the specimens. However, the ingots have the lowest hardnesses and moduli near the surfaces, where cooling during solidification is fastest, while our ribbons are hardest and have highest modulus in regions with the fastest cooling. For ingots, the gradients in hardness are attributed to variations in free volume [2, 3].

What, then, is the cause of the gradient in properties across the ribbons? Clearly, our data exhibit the wrong trend to be explained by local differences in cooling rate. Moreover, the cooling rates across the ribbon are unlikely to differ by more than a factor of 4-7 except immediately adjacent to the wheel surface [13-15], so if we extrapolate 3-5 orders of magnitude down to the cooling rates experienced by ingots, we would predict much larger differences in the properties of ribbons and ingots than are actually observed [4, 5], and the differences are in the wrong direction.

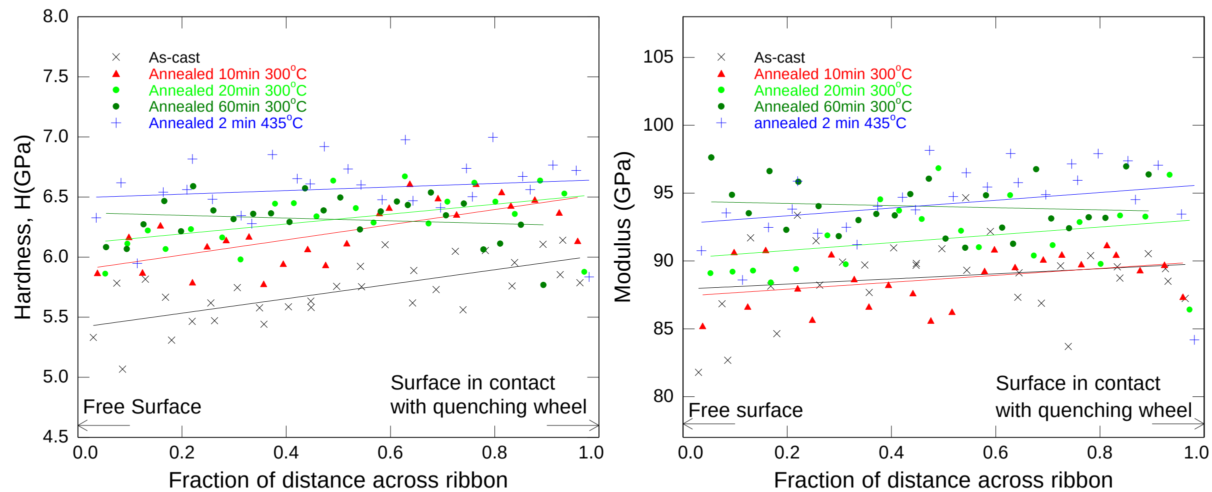

Figure 4. Variation of hardness and modulus across the $Zr_{50}Cu_{45}Al_5$ ribbons under different annealing treatment conditions.

Table I. Summary of the increase in hardness and modulus, and difference in hardness and modulus across the ribbon under different annealing treatments conditions.

	% Change in property at midpoint across the specimen caused by annealing		**% Difference in property across the ribbon** (based on a linear fit)	
	% change in hardness	% change in modulus	% difference in hardness	% difference in modulus
As-cast	0	0	11 ±2	2 ±2
Annealing 300°C, 10 min.	9 ±1	0 ±1	10 ±2	3 ±1
Annealing 300°C, 20 min.	11 ±1	4 ±1	7 ±2	3 ±1
Annealing 300°C, 60 min.	11 ±1	6 ±1	-2 ±2	-1 ±2
Annealing 435°C, 2 min.	16 ±1	7 ±1	6 ±2	3 ±1

One possible cause for a gradient in properties is differences in stress levels across the ribbon, as noted by Liu for ingots [3]. However, this possibility seems contradicted by careful studies showing that stresses influence pileup and sink-in but leave hardness and modulus unaffected when indent areas are measured directly [16, 17], as we have done.

We can rule out a gradient in composition. Energy dispersive spectroscopy (EDS) across the ribbon thickness shows constant composition within 0.5% measurement uncertainty. Also, atomic diffusion coefficients are of the order of 10^{-20} m^2/s^{-1} near T_g [18], which means our annealing experiments would be incapable of making the properties uniform if compositional homogenization were required. Instead, atomic diffusion distances in the annealing experiments were 1-2 nm at most, which is consistent with changes in medium range order and annihilation of free volume. A net decrease in free volume is supported by the decrease in exothermic heat release below T_g in Fig. 1. The gradient in properties across the ribbon thickness might arise from the extreme velocity of the solidification front, on the order of 1 m/s [13]. The front might generate free volume, or alter the distribution of free volume sites, or even push free volume ahead of it, gradually increasing it in the liquid and trapping it in the glass. The last of these processes would accumulate higher free volume toward the surface away from the wheel, consistent with lower hardness and modulus.

CONCLUSIONS

In summary, we have measured gradients in hardness and modulus across the thicknesses of $Zr_{50}Cu_{45}Al_5$ spun ribbons, free from thin-sample artifacts. The hardness of the as-spun ribbon is about 12% higher at the surface in contact with the quenching wheel than at the free surface. Annealing homogenized the hardness and modulus across the ribbons. We hypothesize that the gradient effect is caused by the extreme velocity of the solidification front. Understanding the mechanical properties of rapidly cooled BMG materials subject to large cooling rate gradients may be important for future applications of these materials in very small structures.

This work was supported by the U.S. National science Foundation (CMMI-0824719)

REFERENCES

1. G. Kumar, H.X. Tang, J. Schroers, Nature **457,** 868 (2009).
2. D. Plummer, R. Goodall, I.A. Figueroa, and I. Todd J. of Non-Cryst. Solids. **357,** 814 (2001).
3. Y. Liu, H. Bei, C.T. Liu, and E.P. George, Appl. Phys. Lett. **90,** 71909 (2007).
4. W.H. Jiang, F.X. Liu, Y.D. Wang, H.F. Zhang, H. Choo, and P.K. Liaw, Mater. Sci. Eng. A. **430,** 350 (2006).
5. Z.Y. Liu, Y. Yang, S. Guo, X.J. Liu, J. Lu, Y.H. Liu, and C.T. Liu, J. Alloys Compd. **509,** 3269 (2011).
6. J.E. Jakes, C.R. Frihart, J.F. Beecher, R.J. Moon, P.J. Resto, Z.H. Melgarejo, O.M. Suarez, H. Baumgart, A.A. Elmustafa, and D.S. Stone, J. Mater. Res. **24,** 1016 (2009).
7. J.E. Jakes, C.R. Frihart, J.F. Beecher, R.J. Moon, and D.S. Stone,. J. Mater. Res. **23,** 1113 (2008).
8. I. Kalay, M.J. Kramer, and R.E. Napolitano, Metall. Mater. Trans. A: **42,** 1144 (2011).
9. J. Hwang, Z.H. Melgarejo, Y.E. Kalay, I. Kalay, M.J. Kramer, D.S. Stone, and P.M. Voyles, Phys. Rev. Lett. **108**, 195505 (2012).
10. W.C. Oliver, and G.M. Pharr, J. Mater. Res. **7,** 1564 (1992).
11. A. Bolshakov, and G.M. Pharr, J. Mater. Res. **13,** 1049 (1998).
12. J.E. Jakes, and D.S. Stone, Philos. Mag. **91,** 1387 (2011).
13. A. Zambon, B. Badan, G. Vedovato, and E. Ramous, Mater. Sci. Eng. A . **304,** 592(2001).
14. V.I. Tkatch, S.N. Denisenko, and O.N. Beloshov, Acta Mater. **45,** 2821(1997).
15. V.I. Tkatch, A.I. Limanovskii, S.N. Denisenko, and S.G. Rassolov, Mater. Sci. Eng. A. **323,** 91(2002).
16. T.Y. Tsui, W.C. Oliver, and G.M. Pharr, J. Mater. Res. **11,** (1996) 752.
17. A. Bolshakov, W.C. Oliver, and G.M. Pharr, J. Mater. Res. **11,** 760 (1996).
18. F. Faupel, W. Frank, M.P. Macht, H. Mehrer, V. Naundorf, K. Ratzke, H.R. Schober, S.K. Sharma, and H. Teichler, Rev. Modern Phys. **75,** 237 (2003).